

# An analytic method for quadratic polarons in nonparabolic bands

S. N. Klimin, J. Tempere,<sup>\*</sup> and M. Houtput  
*TQC, Departement Fysica, Universiteit Antwerpen,  
 Universiteitsplein 1, B-2610 Antwerpen, Belgium*

S. Ragni, T. Hahn,<sup>†</sup> and C. Franchini<sup>‡</sup>  
*Faculty of Physics, Computational Materials Physics,  
 University of Vienna, Kolingasse 14-16, Vienna A-1090, Austria*

A. S. Mishchenko<sup>§</sup>  
*Department for Research of Materials under Extreme Conditions,  
 Institute of Physics, 10000 Zagreb, Croatia*

(Dated: July 25, 2024)

## Abstract

Including the effect of lattice anharmonicity on electron-phonon interactions has recently garnered attention due to its role as a necessary and significant component in explaining various phenomena, including superconductivity, optical response, and temperature dependence of mobility. This study focuses on analytically treating the effects of anharmonic electron-phonon coupling on the polaron self-energy, combined with numerical Diagrammatic Monte Carlo data. Specifically, we incorporate a quadratic interaction into the method of squeezed phonon states, which has proven effective for analytically calculating the polaron parameters. Additionally, we extend this method to nonparabolic finite-width conduction bands while maintaining the periodic translation symmetry of the system. Our results are compared with those obtained from Diagrammatic Monte Carlo, partially reported in a recent study [*Phys. Rev. B* **107**, L121109(2023)], covering a wide range of coupling strengths for the nonlinear interaction. Remarkably, our analytic method predicts the same features as the Diagrammatic Monte Carlo simulation.

---

<sup>\*</sup>Also at Lyman Laboratory of Physics, Harvard University, Cambridge, MA 02138, USA.

<sup>†</sup>Center for Computational Quantum Physics, Flatiron Institute, 162 5th Avenue, New York, New York 10010, USA

<sup>‡</sup>Also at Department of Physics and Astronomy “Augusto Righi”, Alma Mater Studiorum – Università di

---

Bologna, Bologna, 40127 Italy

<sup>§</sup>Also at RIKEN Center for Emergent Matter Science (CEMS), Wako, Saitama 351-0198, Japan

## I. INTRODUCTION

Polaron physics, which originates from a theoretical problem that involves the interaction of a particle with a quantum field [1, 2], has garnered significant experimental interest due to its practical applications. This curiosity has additionally driven the advancement of polaron theory, which has broadened its scope from its original concentration on polarons in crystals [3] to include a range of condensed matter systems, such as quantum gases [4–6], and even celestial bodies like neutron stars [7, 8].

Conventional theoretical frameworks for polarons typically center around the idea of small oscillations within a crystal lattice or another bosonic quantum field. Within this framework, the linear-harmonic approximation characterizes the phonon field as harmonic, with the electron-phonon interaction being directly proportional to the phonon coordinates. Instances of such frameworks include the Fröhlich and Holstein models for polarons in solid-state physics [2], as well as Fröhlich-type Hamiltonians for impurity polarons in quantum gases [9]. In these applications, the Fröhlich model relies on the assumption of a parabolic energy dispersion for the conduction band.

It has been established for a while that in certain situations, higher-order terms beyond the linear-harmonic approximation can be significant [10]. These additional terms specifically influence the optical response and kinetics of impurities within crystals. Lately, there has been a resurgence of interest in nonlinear electron-phonon interactions and anharmonic phonons [11–15, 17, 18]. These occurrences have proven crucial in elucidating different phenomena, such as superconductivity at low carrier concentrations [19, 20] and the temperature-dependent mobility [21].

While Diagrammatic Monte Carlo (DiagMC) simulations have made it possible to describe polaron properties for both linear [22, 23] and nonlinear [15] electron-phonon interactions with high accuracy, analytic methods remain of significant interest. These methods provide a clear physical picture of polarons and enhance our understanding of results obtained through numerical techniques such as density functional theory and DiagMC simulations.

The primary objective of the present study is to develop an analytical method for investigating anharmonic polarons within a nonparabolic conduction band characterized by a finite bandwidth. By adjusting the bandwidth and exploring various electron-phonon interaction

amplitudes, this framework encompasses scenarios involving both small and large polarons, as well as the intermediate regime between these extremes. Our approach is based on the well-established method of using displaced squeezed phonon states [24, 25] after elimination of the electron coordinate by a shift to the frame co-moving with the electron [26]. This technique has been widely used for large polarons with linear interactions in weak and intermediate coupling regimes.

One of the important advances in the understanding of the role of high-order terms in the electron-phonon coupling is presented in [16] where the semi-analytic method of momentum average approximation is used to study the Holstein model with simultaneous quadratic and quartic terms. Unfortunately, we cannot verify our results against the data in [16] because we consider a different model, with only quadratic interaction whereas the authors of [16] do not provide results where the quartic term is missing. Also, the paper [16] deals with a polaron in 1D and 2D, while the present work is devoted to a polaron in three dimensions.

In this work, we first extend the displaced squeezed phonon approximation to incorporate quadratic interactions (discussed in Section II). Next, in Section III, we examine polaron behavior with a quadratic interaction in nonparabolic bands while maintaining periodic boundary conditions for the Brillouin zone. This polaron model has been recently explored numerically [15] using the DiagMC technique, and we compare our results with those of DiagMC. Finally, the results obtained are summarized in Section IV.

## II. POLARON WITH FRÖHLICH AND 2TO INTERACTIONS

### A. The system

In this section, we investigate the polaron in a parabolic conduction band, focusing on two distinct types of electron-phonon interactions. Firstly, we examine the Fröhlich interaction, which involves longitudinal optical (LO) phonons and exhibits a linear dependence on phonon coordinates. Secondly, we explore the quadratic interaction which engages two transverse optical (TO) phonons. This 2TO interaction manifests itself as a quadratic function of phonon coordinates. Although the 2TO interaction was introduced in theoretical frameworks long ago [10], it has recently regained interest. Notably, a coexistence of Fröhlich and 2TO couplings has proven relevant in experimental contexts, particularly with materials

such as SrTiO<sub>3</sub> [17, 19, 20]. These interactions have allowed us to successfully elucidate various phenomena, including response properties and superconductivity.

Our analysis centers around the electron-phonon Hamiltonian:

$$H = \frac{\mathbf{p}^2}{2m} + \sum_{a=1}^3 \sum_{\mathbf{q}} \hbar\omega_{\mathbf{q}}^{(a)} b_{\mathbf{q}}^{(a)\dagger} b_{\mathbf{q}}^{(a)} + \sum_{\mathbf{q}} (V_{\mathbf{q}} b_{\mathbf{q}}^{(3)} e^{i\mathbf{q}\cdot\mathbf{r}} + V_{\mathbf{q}}^* b_{\mathbf{q}}^{\dagger(3)} e^{-i\mathbf{q}\cdot\mathbf{r}}) + H_{2\text{TO}} \quad (1)$$

Here,  $\mathbf{r}$  is the position operator of the electron with band mass  $m$ ,  $\mathbf{p}$  is its canonically conjugate momentum operator;  $b_{\mathbf{q}}^{\dagger(a)}$  and  $b_{\mathbf{q}}^{(a)}$  are the creation and annihilation operators for optical phonons of wave vector  $\mathbf{q}$  and energy  $\hbar\omega_{\mathbf{q}}^{(a)}$ . The index  $a = 1, 2$  labels the TO phonon modes, and  $a = 3$  denotes the LO mode. So further on in this note we assume that  $\omega_{\mathbf{q}}^{(1)} = \omega_{\mathbf{q}}^{(2)} = \omega_{\mathbf{q}}^{(\text{TO})}$  and  $\omega_{\mathbf{q}}^{(3)} = \omega_{\text{LO}}$ . The  $V_{\mathbf{q}}$  are Fourier components of the linear (Fröhlich) part of the electron-phonon interaction

$$V_{\mathbf{q}} = \frac{\hbar\omega_{\text{LO}}}{q} \left( \frac{4\pi\alpha}{V} \right)^{\frac{1}{2}} \left( \frac{\hbar}{2m\omega_{\text{LO}}} \right)^{\frac{1}{4}}. \quad (2)$$

The strength of the Fröhlich electron-phonon interaction is expressed by a dimensionless coupling constant  $\alpha$ , which is defined as:

$$\alpha = \frac{e^2}{\hbar} \sqrt{\frac{m}{2\hbar\omega_{\text{LO}}}} \left( \frac{1}{\varepsilon_{\infty}} - \frac{1}{\varepsilon_0} \right). \quad (3)$$

In this definition,  $\varepsilon_{\infty}$  and  $\varepsilon_0$  are, respectively, the high-frequency and static dielectric constants of the polar crystal.

We apply the quadratic electron-phonon interaction Hamiltonian following Ref. [13]:

$$H_{2\text{TO}} = \frac{g_2}{2} \vec{P}^2(\mathbf{r}) \quad (4)$$

where  $g_2$  is the coupling strength for the 2TO interaction. The polarization  $\vec{P}(\mathbf{r})$  is given by

$$\vec{P}(\mathbf{r}) = \sum_{\mathbf{q}} \sum_{a=1,2} \frac{\mathbf{e}_{\mathbf{q}}^{(a)}}{\sqrt{V}} \varkappa_{\mathbf{q}} (b_{\mathbf{q}}^{(a)} e^{i\mathbf{q}\cdot\mathbf{r}} + b_{\mathbf{q}}^{(a)\dagger} e^{-i\mathbf{q}\cdot\mathbf{r}}) \quad (5)$$

with the factor to the interaction strength,

$$\varkappa_{\mathbf{q}} = \sqrt{\omega_{\mathbf{q}}^{(\text{TO})} \frac{\varepsilon_0(\mathbf{q}) - \varepsilon_{\infty}}{4\pi}} \quad (6)$$

where  $\varepsilon_0(\mathbf{q})$  and  $\varepsilon_{\infty}$  are, respectively, the static momentum-dependent dielectric function and high-frequency dielectric constant. In the considered isotropic model, there are two unit vectors  $\mathbf{e}_{\mathbf{q}}^a$  for TO modes, with  $a = 1, 2$ , orthogonal to  $\mathbf{q}$  and to each other.

## B. The approximation of squeezed phonon states

The original idea of the Lee-Low-Pines transformation [26] followed by the Bogoliubov-Tyablikov diagonalization [27] of the truncated coordinate-free polaron Hamiltonian, quadratic in phonon coordinates, belongs to Gross [24]. This approximation was subsequently further developed in different modifications, e.g., the method of displaced squeezed phonon states [25] or correlated Gaussian wave functions [6] (see also Refs. [28–30]). Here, we show that the approximation of displaced squeezed phonon states (abbreviated to SPS in the figures) is straightforwardly extended to a polaron with a quadratic electron-phonon interaction.

The first Lee-Low-Pines unitary transformation

$$S_1 = \exp \left[ \frac{i}{\hbar} \left( \mathbf{P} - \sum_{a,\mathbf{q}} \hbar \mathbf{q} b_{\mathbf{q}}^{(a)\dagger} b_{\mathbf{q}}^{(a)} \right) \cdot \mathbf{r} \right], \quad (7)$$

where  $\mathbf{P}$  is the eigenvalue of the total momentum, leads to the coordinate-free polaron Hamiltonian

$$\begin{aligned} \mathcal{H} &= S_1^{-1} H S_1 \\ &= \frac{\left( \mathbf{P} - \sum_{a,\mathbf{q}} \hbar \mathbf{q} b_{\mathbf{q}}^{(a)\dagger} b_{\mathbf{q}}^{(a)} \right)^2}{2m} + \sum_{a=1}^3 \sum_{\mathbf{q}} \hbar \omega_{\mathbf{q}}^{(a)} b_{\mathbf{q}}^{(a)\dagger} b_{\mathbf{q}}^{(a)} \\ &\quad + \sum_{\mathbf{q}} V_{\mathbf{q}} B_{\mathbf{q}}^{(3)} + \frac{g_2}{2V} \left( \sum_{\mathbf{q},a} \varkappa_{\mathbf{q}} \mathbf{e}_{\mathbf{q}}^{(a)} B_{\mathbf{q}}^{(a)} \right)^2. \end{aligned} \quad (8)$$

Here  $B_{\mathbf{q}}^{(a)}$  is proportional to the phonon coordinate, and is given by

$$B_{\mathbf{q}}^{(a)} = b_{\mathbf{q}}^{(a)} + b_{\mathbf{q}}^{(a)\dagger}. \quad (9)$$

The coordinate-free Hamiltonian looks appealing for approximate methods and led to numerous attempts to make analytic approximations suitable at both weak and strong coupling. Here, we consider the well-established approach for the weak- and intermediate-coupling regime. In this approach, the second Lee-Low-Pines transformation is performed,

$$S_2 = \exp \left[ - \sum_{a,\mathbf{q}} f_{\mathbf{q}}^{(a)} (b_{\mathbf{q}}^{(a)} - b_{\mathbf{q}}^{(a)\dagger}) \right]. \quad (10)$$

The phonon shifts  $f_{\mathbf{q}}^{(a)}$  are real, in accordance with the polaron Hamiltonian. The unitary transformation  $S_2$  results in a displacement of the phonon operators. The resulting

transformed Hamiltonian consists of two terms:

$$S_2^{-1} \mathcal{H} S_2 = H_0 + H_I$$

where  $H_0$  and  $H_I$  are the following contributions to the coordinate-free Hamiltonian after phonon shifts:

(1) The Hamiltonian truncated to the quadratic normal form of phonon operators:

$$H_0 = E_0 + \sum_{a, \mathbf{q}} \hbar \Omega_{\mathbf{q}}^{(a)} b_{\mathbf{q}}^{(a)\dagger} b_{\mathbf{q}}^{(a)} + \frac{1}{2m} \left( \sum_{a, \mathbf{q}} \hbar \mathbf{q} f_{\mathbf{q}}^{(a)} B_{\mathbf{q}}^{(a)} \right)^2 + \frac{g_2}{2V} \left( \sum_{\mathbf{q}, a=1,2} \mathbf{e}_{\mathbf{q}}^{(a)} \chi_{\mathbf{q}} B_{\mathbf{q}}^{(a)} \right)^2 \quad (11)$$

with the renormalized phonon energy,

$$\hbar \Omega_{\mathbf{q}}^{(a)} = \hbar \omega_{\mathbf{q}}^{(a)} + \frac{\hbar^2 \mathbf{q}^2}{2m} - \frac{\hbar (\mathbf{q} \cdot \mathbf{P})}{m} + \sum_{a', \mathbf{q}'} \frac{\hbar^2}{m} (\mathbf{q} \cdot \mathbf{q}') (f_{\mathbf{q}'}^{(a')})^2 \quad (12)$$

where the term  $E_0$  does not contain operators:

$$E_0 = \frac{\mathbf{P}^2}{2m} + \sum_{a, \mathbf{q}} \left( \hbar \omega_{\mathbf{q}}^{(a)} - \frac{(\hbar \mathbf{q} \cdot \mathbf{P})}{m} \right) (f_{\mathbf{q}}^{(a)})^2 + 2 \sum_{\mathbf{q}} V_{\mathbf{q}} f_{\mathbf{q}}^{(3)} + \frac{1}{2m} \left( \sum_{a, \mathbf{q}} \hbar \mathbf{q} (f_{\mathbf{q}}^{(a)})^2 \right)^2 + \frac{2g_2}{V} \left( \sum_{\mathbf{q}, a=1,2} \mathbf{e}_{\mathbf{q}}^{(a)} \chi_{\mathbf{q}} f_{\mathbf{q}}^{(a)} \right)^2, \quad (13)$$

(2) The remaining part of the Hamiltonian, which is also written in the normal form:

$$H_I = \sum_{\mathbf{q}} (\hbar \Omega_{\mathbf{q}}^{(3)} f_{\mathbf{q}}^{(3)} + V_{\mathbf{q}}) B_{\mathbf{q}}^{(3)} + \sum_{\mathbf{q}, a=1,2} \left( \hbar \Omega_{\mathbf{q}}^{(a)} f_{\mathbf{q}}^{(a)} + \frac{2g_2}{V} \sum_{\mathbf{q}', a'=1,2} (\mathbf{e}_{\mathbf{q}}^{(a)} \cdot \mathbf{e}_{\mathbf{q}'}^{(a')}) \chi_{\mathbf{q}} \chi_{\mathbf{q}'} f_{\mathbf{q}'}^{(a')} \right) B_{\mathbf{q}}^{(a)} + \sum_{a, \mathbf{q}} \sum_{a', \mathbf{q}'} \frac{\hbar^2 (\mathbf{q} \cdot \mathbf{q}')}{m} f_{\mathbf{q}}^{(a)} b_{\mathbf{q}'}^{(a')\dagger} B_{\mathbf{q}}^{(a)} b_{\mathbf{q}'}^{(a')} + \sum_{a, \mathbf{q}} \sum_{a', \mathbf{q}'} \frac{\hbar^2 (\mathbf{q} \cdot \mathbf{q}')}{2m} b_{\mathbf{q}}^{(a)\dagger} b_{\mathbf{q}'}^{(a')\dagger} b_{\mathbf{q}}^{(a)} b_{\mathbf{q}'}^{(a')}. \quad (14)$$

The term  $H_I$  can only quantitatively influence the polaron energy in a sufficiently strong coupling. Consequently, an account of this contribution is beyond the scope of the present work, which is restricted to weak- and intermediate-coupling regimes.

### C. 2TO polaron self-energy

The Hamiltonian  $H_0$ , given by Eq. (11), is quadratic in the phonon operators, but it does contain products of two creation or two annihilation operators. Such Hamiltonians can be diagonalized by a Bogoliubov transformation, which can be interpreted as a unitary transformation representing a phonon *squeezing*. We refer to this transformation as the Bogoliubov-Tyablikov diagonalization [27]. The momentum-dependent polaron energy shift provided by the Bogoliubov-Tyablikov diagonalization is found starting from the definition [31]

$$\Delta E = \frac{1}{2} \sum_{a,\mathbf{q}} \hbar (\nu_{\mathbf{q}}^{(a)} - \Omega_{\mathbf{q}}^{(a)}), \quad (15)$$

where  $\nu_{\mathbf{q}}^{(a)}$  are eigenfrequencies determined in Appendix A which satisfy Eq. (A26). In fact, the energy  $\Delta E$  is calculated exactly without the necessity to know the eigenfrequencies explicitly – the details are described in Appendix A. The resulting polaron self-energy consists of (13) and the self-energy correction due to the squeezing transformation,

$$E_p(\mathbf{P}) = E_0 + \Delta E. \quad (16)$$

Polarons of different types with linear electron-phonon coupling within the displaced squeezed phonon approximation were extensively studied in earlier work, e.g. [6, 24, 28, 29]. Therefore, here we focus only on the self-energy of the 2TO polaron. To understand the effects of quadratic coupling more clearly, we restrict the results analysis to the case of a purely quadratic polaron without linear electron-phonon interaction. In general, when both linear and quadratic interactions are present in the Hamiltonian,  $f_{\mathbf{q}}^{(a)}$  are treated as variational functions and are chosen to minimize the polaron self-energy (16). In the absence of linear coupling, the optimal phonon shift values appear to be zero. Thus, the polaron energy shift for a purely quadratic polaron is only expressed by the term  $\Delta E$ . It is derived using the known scheme of the meson pair theory [31] and expressed through the contour integral

$$\Delta E^{(2\text{TO})}(P) = -\frac{\hbar}{8\pi i} \oint_C ds \frac{1}{\sqrt{s}} \ln \Delta^{(2\text{TO})}(s, P) \quad (17)$$

with the function (see Appendix A)

$$\ln \Delta^{(2\text{TO})}(s, P) = \sum_{j=x,y,z} \ln \left[ 1 - \frac{g_2}{\hbar V} \sum_{\mathbf{q}, a=1,2} \left( 1 - \frac{q_j^2}{q^2} \right) \frac{\varkappa_{\mathbf{q}}^2 \Omega_{\mathbf{q}}^{(a)}}{s - (\Omega_{\mathbf{q}}^{(a)})^2} \right]. \quad (18)$$



The integration contour  $C$  contains inside all values of  $(\nu_{\mathbf{q}}^{(a)})^2$  and  $(\Omega_{\mathbf{q}}^{(a)})^2$  as shown in Fig. 1.

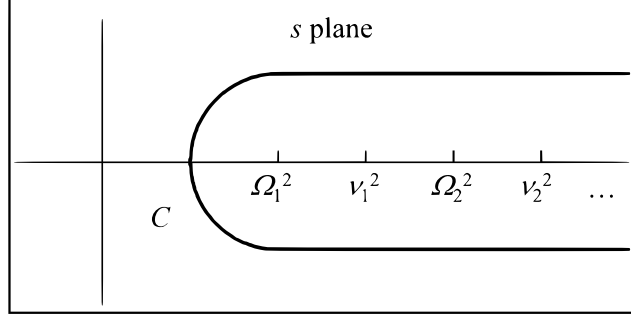


FIG. 1: Integration contour in the complex  $s$  plane for the polaron energy shift.

Here, for numeric testing, we use the approximation of a soft TO mode applied by Kumar *et al.* [13]:

$$\omega_{\mathbf{q}}^{(\text{TO})} = \sqrt{\omega_T^2 + c^2 q^2}$$

and neglect  $\omega_{\mathbf{q}}^{(\text{TO})}\big|_{q=0} = \omega_T$  with respect to  $cq$ . Thus the soft mode is approximately sound-like:

$$\omega_{\mathbf{q}}^{(\text{TO})} \approx cq, \quad \varkappa_{\mathbf{q}}^2 \approx \frac{\varepsilon_{\infty} \omega_{\text{LO}}^2}{4\pi cq} \quad (19)$$

Without knowledge of a realistic large- $q$  behavior of the TO-phonon energy and of the 2TO interaction, the integrals over the phonon momentum in the present approximation diverge. To remove this divergence a phonon wave vector cutoff  $k_0$  is introduced. The coupling strength of the 2TO interaction is expressed through the dimensionless coupling constant

$$\alpha_T = g_2 \frac{\varepsilon_{\infty} m \omega_{\text{LO}}^2}{6\pi^3 \hbar^2 c}. \quad (20)$$

The polaron energy shift (17) describes the dispersion of the polaron  $\Delta E^{(2\text{TO})}(P)$  as a function of the polaron momentum  $P$ . The numeric results for this 2TO contribution to the polaron self-energy are shown in Fig. 2. The polaron energies  $\Delta E^{(2\text{TO})}$  are plotted as functions of the total momentum  $P$  for different values of the coupling constant  $\alpha_T$ . The numeric calculation is performed using the units with  $\hbar = 1$ ,  $m = 1$ , and  $c = 1$ . Thus the energy is measured in units of  $mc^2$ .

To our knowledge, the sign of the coupling constant for the 2TO interaction is not known *a priori*. Therefore, the polaron self-energy is calculated here for both positive and negative

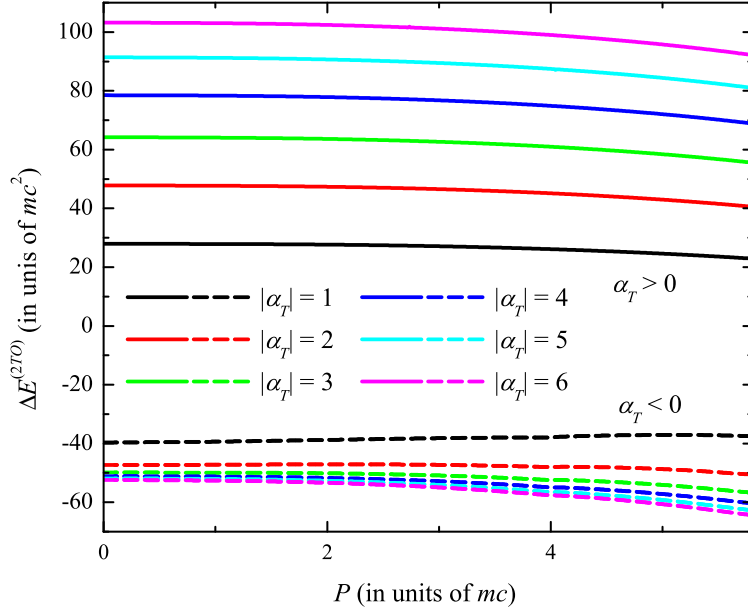


FIG. 2: Momentum-dependent TO2-polaron energy shift as a function of the polaron momentum  $P$  for different values of the coupling constant  $\alpha_T$ , calculated using the momentum cutoff  $\hbar k_0 = 10mc$ . Solid and dashed curves show the energy for positive and negative  $\alpha_T$ , respectively.

$\alpha_T$ , shown by solid and dashed curves, respectively. The range of the polaron momentum is chosen sufficiently small with respect to the momentum cutoff in order to avoid possible artifacts related to the cutoff. As can be seen in Fig. 2, the 2TO polaron energy shift  $\Delta E^{(2TO)}(P)$  smoothly and monotonically decreases as a function of  $P$ .

Expanding the momentum-dependent 2TO polaron energy shift (17) in powers of  $P$  up to the second order, we obtain the ground state energy and the polaron contribution to the inverse effective mass for the 2TO polaron. The ground state energy  $\Delta E^{(2TO)}(P)$  is plotted in Fig. 3. Results of the present method are labeled “SPS” which stands for the “squeezed phonon state” approach, since that is indeed what we rely on through the Bogoliubov-Tyablikov diagonalization.

The polaronic energy shift resulting from the 2TO interaction depends not only on the magnitude of the interaction but also on its sign. For  $\alpha_T > 0$ , its behavior resembles the repulsive polaron in atomic quantum gases [5]. The dependence of the self-energy on  $\alpha_T$  is not fully antisymmetric when changing the sign of  $\alpha_T$ , because both even and odd terms contribute to the total energy.

The dashed lines show the first-order perturbation result for the ground state energy

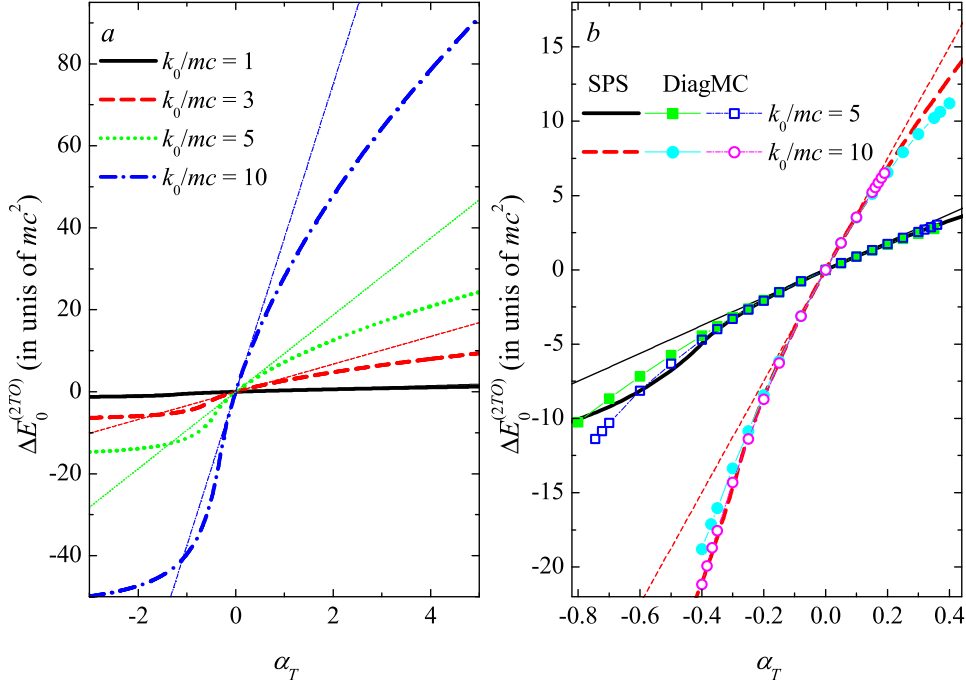


FIG. 3: (a) TO2-polaron ground state energy calculated using the approximations for the soft-mode TO-phonon dispersion and the coupling factor by Kumar *et al.* [13] for different values of the phonon cutoff momentum  $k_0$ . The thin lines show the first-order perturbation results for  $E^{(2TO)}$ . (b) The ground state polaron energy within the approximation of squeezed phonon states compared with results of partial summation of DiagMC series containing up to 2-loop diagrams (filled symbols) and up to 3-loop diagrams (hollow symbols). Errorbars of DiagMC data are smaller than the points size.

determined by the averaging of the electron-phonon interaction term with the Hamiltonian of free electrons and phonons,

$$E_{weak}^{(2TO)} = \langle H_{2TO} \rangle_0 = \frac{3 \hbar^2 k_0^2}{8 m} \alpha_T. \quad (21)$$

The ground state energy determined from (17) at  $P = 0$  analytically tends to  $\langle H_{2TO} \rangle_0$  in the limit of small coupling constant  $\alpha_T$ .

The dependence of the effective mass on the coupling constant  $\alpha$  is shown in Fig. 4. For a positive coupling constant, the  $\alpha_T$  dependence of the effective mass is smooth and does not manifest any specific feature. The 2TO polaron effective mass monotonically rises with an increasing  $\alpha_T$ , as well as with an increasing phonon cutoff momentum  $k_0$ .

The behavior of the effective mass at negative  $\alpha_T$  is more interesting. It exhibits a reso-

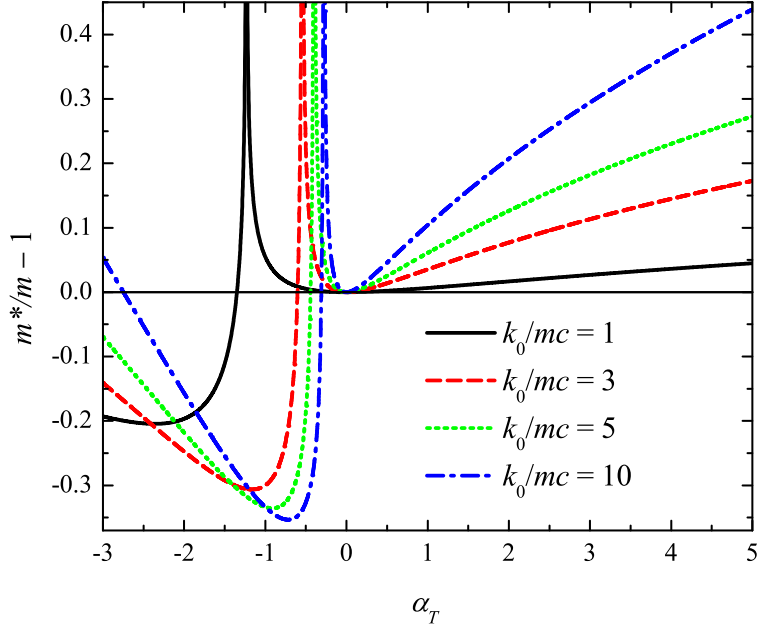


FIG. 4: TO2-polaron effective mass as a function of the coupling constant  $\alpha_T$ , calculated using different values of the momentum cutoff  $k_0$ .

nant divergent peak of the effective mass at some value of  $\alpha_T$ . A divergence of the effective polaron mass at some negative coupling strength of the quadratic interaction was also obtained in our preceding work on a polaron in a finite-width band [15] using the numerically exact Diagrammatic Monte Carlo method. This result has been verified analytically in the case of an infinitely narrow conduction band, which is known as the *atomic limit*, also discussed in the next section. The atomic limit results in an explicit analytic change of the phonon frequency. When the coupling constant passes through a certain critical negative value, this renormalized squared phonon frequency becomes negative, which indicates a negative stiffness and an instability of the crystal lattice possibly resulting in a structural phase transition. At the critical coupling strength, the polaron effective mass diverges. Consequently, this also means an instability of the polaron state.

When the width of the conduction band is not equal to zero, the effect of the quadratic coupling is more complicated and can hardly be reduced to a renormalization of the phonon frequency. Nevertheless, it is physically clear that a quadratic polaron with any band width should become unstable when the coupling strength reaches a sufficiently large negative value. This must be also true for the polaron model with a parabolic electron dispersion treated in this section. Therefore, the divergence of the polaron effective mass shown in Fig.

4 is attributed to the polaron instability. The present approximation of squeezed phonon states gives formal solutions for coupling strengths both above and below this critical value (denoted as  $\alpha_T^{(c)}$ ). However, we should only consider the range  $\alpha_T > \alpha_T^{(c)}$  as physically reasonable.

It should be noted that an account of a whole series of anharmonic terms in the phonon Hamiltonian (see also discussions in Refs. [16, 32]) might avoid this polaron instability, which may appear as an artifact of restricting the phonon Hamiltonian to the quadratic order. However, even in this case the instability would be an artifact of the quadratic polaron model but not an artifact of the approximation of squeezed phonon states, because, as shown in the next section, the DiagMC calculation and the approximation of squeezed phonon states predict the same divergence of the polaron effective mass.

As was proven by Gerlach and Löwen [33] who considered rigorous relations for a polaron, “phase transitions” when varying the coupling strength are forbidden for a rather wide class of polarons, which however do not include all existing polaron models. Gerlach and Löwen considered polarons with a linear electron-phonon coupling, where the coupling amplitude depends only on the phonon momentum. The theorem can be inapplicable even for a nonlocal linear electron-phonon interaction, for example, the Peierls/Su-Schrieffer-Heeger polaron [34] or for a polaron exposed to a short-range potential [33]. Furthermore, polarons with nonlinear electron-phonon interactions were beyond the scope of the study in Ref. [33].

The polaron with a quadratic electron-phonon coupling of Ref. [15] represents an example of an exactly solvable polaron model in the atomic limit. It shows that the Gerlach-Löwen theorem can be inapplicable in the case of a quadratic interaction.

Remarkably, there are kinks (discontinuities of the first derivative) in the curve for the ground state energy in Fig. 3 at the same critical values of the coupling constant where the 2TO polaron effective mass diverges. As discussed above and in Sec. III, the physical origin of these features consists in the polaron instability which appears when the coupling strength of the quadratic interaction reaches some critical negative value  $\alpha_T^{(c)}$ . In the parameter range for  $\alpha > \alpha_T^{(c)}$ , the result of the approximation of squeezed phonon states is well consistent with DiagMC simulations (Fig. 3 (b)) of a subset of the diagrammatic expansion of the polaron Green function. The terms involved are all crossing diagrams containing 2-loops and 3-loops, which are the dominant contribution at small coupling. The inclusion of 3-loops results in a behavior closer to the squeezed phonon state result compared to 2-loops

alone. The implementation of the DiagMC method is described in Appendix B.

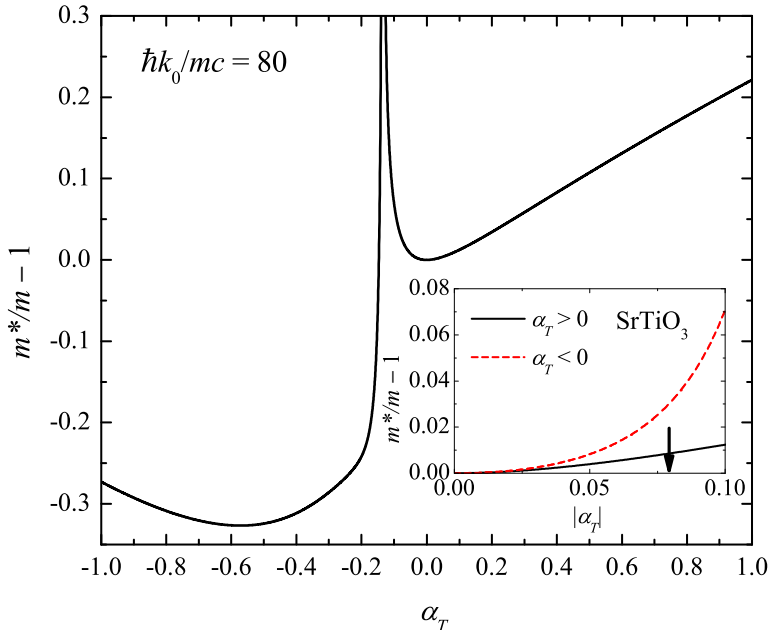


FIG. 5: TO2-polaron effective mass as a function of the coupling constant  $\alpha_T$ , calculated using the momentum cutoff  $\hbar k_0 = 80mc$ , which approximately corresponds to the Brillouin zone edge in SrTiO<sub>3</sub>. *Inset*: the effective mass in the weak-coupling range of  $\alpha_T$ . The arrow indicates the value  $\alpha_T \approx 0.079$  obtained using the parameters from Ref. [13].

In Fig. 5, the 2TO polaron effective mass is shown as a function of  $\alpha_T$  choosing other parameters the same as in Ref. [13] in order to see whether the 2TO interaction may be relevant for polarons in strontium titanate. Kumar *et al.* use  $g_2$  as a fitting parameter, and apply for numerics  $g_2 = 0.92a_0^3$  where  $a_0$  is the lattice constant taken in Ref. [13] to be  $a_0 = 3.9 \text{ \AA}$ . With other parameters from the same work,  $c = 6.6 \times 10^5 \text{ cm s}^{-1}$ , the bare electron band mass  $m = 1.8m_0$  (where  $m_0$  is the electron mass in vacuum), and with  $\hbar\omega_{\text{LO}} = 0.0987 \text{ eV}$  [35], we estimate the dimensionless 2TO coupling constant in SrTiO<sub>3</sub> as  $\alpha_T \approx 0.079$ . This value is indicated by the arrow in the inset of Fig. 5. The phonon cutoff momentum is chosen here as the edge of the Brillouin zone,  $k_0 = \pi/a_0$ , which gives us the dimensionless cutoff value  $p_0 = \hbar k_0/mc \approx 80$ .

As can be seen from Fig. 5, the relative contribution of the 2TO interaction to the polaron mass in SrTiO<sub>3</sub> is relatively small with respect to the Fröhlich polaron mass, which can be estimated as  $m_F^*/m - 1 \approx \alpha/6 \approx 0.35$  [35]. However the 2TO contribution is not negligible. Moreover, if it may appear that the coupling constant in SrTiO<sub>3</sub> is negative, the value

$|\alpha_T| \approx 0.079$  lies rather close to the resonance obtained in the present calculation. This may explain larger values for the effective mass of a “dressed” electron obtained in spectroscopic measurements with respect to that which follows from our calculations (predicting  $\alpha \approx 2.1$ ).

Figs. 4 and 5 show that the critical negative coupling  $\alpha_T^{(c)}$  gradually decreases in magnitude when increasing the momentum cutoff  $k_0$ . If the cutoff value tends to infinity, it means physically an infinite increase of a negative contribution to the renormalized squared phonon frequency at any finite  $\alpha_T$ . Thus we can suggest that in the limit  $k_0 \rightarrow \infty$ , the critical coupling constant  $\alpha_T^{(c)}$  must tend to zero.

### III. INCLUDING NONPARABOLICITY AND FINITE WIDTH OF THE CONDUCTION BAND

#### A. Model

The most important point of this subsection consists in a generalization of the method using displaced squeezed phonon states to the polaron in a nonparabolic finite-width conduction band. The generalized method satisfies periodic boundary conditions in the Brillouin zone and consequently it is not restricted to a small polaron momentum. Thus, it allows for a description of both large and small polarons.

The treatment in the present work is performed for the polaron model introduced in Ref. [15]. The polaron problem is treated using the Hamiltonian in the lattice representation for a simple cubic lattice, written as  $H = H_0 + H_{e-ph}$  where

$$H_0 = -t \sum_{\langle i', i \rangle} \sum_{\sigma=\pm 1/2} c_{i',\sigma}^\dagger c_{i,\sigma} + \sum_{i', i} \omega_0 \left( b_{i'}^\dagger b_i + \frac{1}{2} \right), \quad (22)$$

$$H_{e-ph} = \frac{\omega_0}{4} g \sum_{\mathbf{i}} n_{\mathbf{i}} B_{\mathbf{i}}^2, \quad (23)$$

with

$$B_{\mathbf{i}} = b_{\mathbf{i}} + b_{\mathbf{i}}^\dagger, \quad (24)$$

$$n_{\mathbf{i}} = \sum_{\sigma=\pm 1/2} c_{\mathbf{i},\sigma}^\dagger c_{\mathbf{i},\sigma}. \quad (25)$$

In reciprocal space the lattice corresponds to a discrete finite set of wave vectors,

$$-\frac{\pi}{a_0} \leq (k_j, q_j) < \frac{\pi}{a_0}, \quad (k_j, q_j) = \frac{2\pi i_j}{L} \quad (j = x, y, z), \quad (26)$$

where  $L = N^{1/3}a_0$  is the size of the system ( $V = L^3 = Na_0^3$ ),  $a_0$  being the lattice constant, and  $i_j$  are integers.

In the momentum representation, applying the discrete Fourier transform

$$c_{\mathbf{i},\sigma} = \frac{1}{N^{1/2}} \sum_{\mathbf{k}} c_{\mathbf{k},\sigma} e^{i\mathbf{k}\cdot\mathbf{r}_i}, \quad c_{\mathbf{i},\sigma}^\dagger = \frac{1}{N^{1/2}} \sum_{\mathbf{k}} c_{\mathbf{k},\sigma}^\dagger e^{-i\mathbf{k}\cdot\mathbf{r}_i}, \quad (27)$$

$$B_{\mathbf{q}} = \frac{1}{N^{1/2}} \sum_{\mathbf{i}} e^{-i\mathbf{q}\cdot\mathbf{r}_i} B_{\mathbf{i}}, \quad B_{\mathbf{i}} = \frac{1}{N^{1/2}} \sum_{\mathbf{q}} e^{i\mathbf{q}\cdot\mathbf{r}_i} B_{\mathbf{q}}, \quad (28)$$

the Hamiltonian  $H_0$  takes the form

$$H_0 = \sum_{\mathbf{k}} \varepsilon(\mathbf{k}) \sum_{\sigma} c_{\mathbf{k},\sigma}^\dagger c_{\mathbf{k},\sigma} + \sum_{\mathbf{q}} \omega_0 \left( b_{\mathbf{q}}^\dagger b_{\mathbf{q}} + \frac{1}{2} \right) \quad (29)$$

with  $\varepsilon(\mathbf{k})$  (counted from the middle of the conduction band) given by

$$\varepsilon(\mathbf{k}) = -2t \sum_{j=x,y,z} \cos(k_j a_0). \quad (30)$$

The quadratic interaction Hamiltonian becomes

$$H_{e-ph} = \frac{\omega_0}{4} g \frac{1}{N} \sum_{\mathbf{q}} \sum_{\mathbf{q}'} \sum_{\mathbf{k}} \sum_{\sigma} c_{\mathbf{k}+\mathbf{q}-\mathbf{q}',\sigma}^\dagger c_{\mathbf{k},\sigma} B_{\mathbf{q}} B_{\mathbf{q}'}^\dagger \quad (31)$$

with  $B_{\mathbf{q}} = b_{\mathbf{q}} + b_{-\mathbf{q}}^\dagger$ .

Expanding the band dispersion up to quadratic order,  $\varepsilon(\mathbf{k}) = a_0^2 t k^2 + O(k^4)$ , yields the relation between the bandwidth parameter  $t$  and the band mass  $m_b$ :

$$t = \frac{\hbar^2}{2m_b a_0^2}, \quad m_b = \frac{\hbar^2}{2a_0^2 t} \quad (32)$$

The band width for the tight-binding model is  $W \equiv \max[\varepsilon(\mathbf{k})] - \min[\varepsilon(\mathbf{k})] = 12t$ . Further on, we set  $\hbar = 1$ . The other units will be set below.

For a single polaron, the parts of the single-polaron Hamiltonian are

$$H_0(\mathbf{p}, \{b_{\mathbf{q}}^\dagger, b_{\mathbf{q}}\}) = \varepsilon(\mathbf{p}) + \sum_{\mathbf{q}} \omega_0 \left( b_{\mathbf{q}}^\dagger b_{\mathbf{q}} + \frac{1}{2} \right), \quad (33)$$

$$H_{e-ph}(\mathbf{r}, \{b_{\mathbf{q}}^\dagger, b_{\mathbf{q}}\}) = \frac{\omega_0}{4} g \frac{1}{N} \sum_{\mathbf{q}} \sum_{\mathbf{q}'} e^{i(\mathbf{q}-\mathbf{q}')\cdot\mathbf{r}} B_{\mathbf{q}} B_{\mathbf{q}'}^\dagger. \quad (34)$$

The first Lee-Low-Pines transformation, as in Sec. II, leads to an electron coordinate-free Hamiltonian. In order to apply the Bogoliubov-Tyablikov transformation, this Hamiltonian is rewritten in terms of real phonon coordinates,

$$\mathcal{H} = \varepsilon(\mathbf{P} - \mathbf{Q}) + \sum_{\mathbf{q}} \omega_0 \left( b_{\mathbf{q}}^\dagger b_{\mathbf{q}} + \frac{1}{2} \right) + \frac{\omega_0 g}{4N} \left( \sum_{\mathbf{q}} (b_{\mathbf{q}} + b_{\mathbf{q}}^\dagger) \right)^2, \quad (35)$$



where the total phonon momentum is  $\mathbf{Q} = \sum_{\mathbf{q}} \mathbf{q} b_{\mathbf{q}}^{\dagger} b_{\mathbf{q}}$ . Representing  $\varepsilon(\mathbf{P} - \mathbf{Q})$  through the normal products of phonon second quantization operators, we arrive at the result:

$$\begin{aligned} \varepsilon(\mathbf{P} - \mathbf{Q}) = & -t \sum_{j=1}^3 \left[ e^{ia_0 P_j} \mathbf{N} \exp \left( \sum_{\mathbf{q}} (e^{-ia_0 q_j} - 1) b_{\mathbf{q}}^{\dagger} b_{\mathbf{q}} \right) \right. \\ & \left. + e^{-ia_0 P_j} \mathbf{N} \exp \left( \sum_{\mathbf{q}} (e^{ia_0 q_j} - 1) b_{\mathbf{q}}^{\dagger} b_{\mathbf{q}} \right) \right]. \end{aligned} \quad (36)$$

where  $\mathbf{N}(\dots)$  denotes the normal form of second quantization operators. When truncating the Taylor series of (36) in powers of normal products of phonon operators up to the quadratic order, this gives us the expression

$$\varepsilon^{(quad)}(\mathbf{P} - \mathbf{Q}) = \varepsilon(\mathbf{P}) + \sum_{\mathbf{q}} [\varepsilon(\mathbf{P} - \mathbf{q}) - \varepsilon(\mathbf{P})] b_{\mathbf{q}}^{\dagger} b_{\mathbf{q}}. \quad (37)$$

Consequently, the Hamiltonian (35) can be subdivided in the two parts

$$\mathcal{H} = H_0 + H_I \quad (38)$$

where the Hamiltonian  $H_0$  is a quadratic form of phonon operators,

$$H_0 = \varepsilon(\mathbf{P}) + \sum_{\mathbf{q}} \frac{\omega_0}{2} + \sum_{\mathbf{q}} \Omega_{\mathbf{q}} b_{\mathbf{q}}^{\dagger} b_{\mathbf{q}} + \frac{\omega_0 g}{4N} \left( \sum_{\mathbf{q}} (b_{\mathbf{q}} + b_{\mathbf{q}}^{\dagger}) \right)^2, \quad (39)$$

with the renormalized phonon frequency  $\Omega_{\mathbf{q}}$ ,

$$\Omega_{\mathbf{q}} = \omega_0 + \varepsilon(\mathbf{P} - \mathbf{q}) - \varepsilon(\mathbf{P}), \quad (40)$$

and  $H_I$  is a series of all higher-order terms beyond the quadratic expansion,

$$H_I = \varepsilon(\mathbf{P} - \mathbf{Q}) - \varepsilon^{(quad)}(\mathbf{P} - \mathbf{Q}). \quad (41)$$

As can be explicitly seen from (36), both the total Hamiltonian  $\mathcal{H}$  and the quadratic Hamiltonian  $H_0$  have the correct periodic translation symmetry, the same as for the initial exact electron-phonon Hamiltonian. Namely,  $\varepsilon(\mathbf{P})$ ,  $\varepsilon(\mathbf{P} - \mathbf{Q})$  and  $\Omega_{\mathbf{q}}$  are invariant with respect to the periodic translations  $P_j \rightarrow P_j + 2\pi/a_0$  and/or  $q_j \rightarrow q_j + 2\pi/a_0$ . Consequently, the present scheme exactly accounts for the boundary conditions of the Brillouin zone both for an electron and phonons. When including both linear and quadratic electron-phonon interactions, the full expansion of the kinetic energy in powers of phonon operators is performed in the same way without difficulties. Therefore this expansion gives us the straightforward extension of the method of squeezed phonon states to a polaron in a non-parabolic finite-width band. As a particular case, this provides the equivalent scheme of displaced squeezed phonon approach for a small polaron.

## B. Self-energy of a polaron with a quadratic interaction

The shift of the self-energy provided by the Bogoliubov-Tyablikov diagonalization is determined in the same way as in Sec. II and gives

$$\Delta E(\mathbf{P}) = -\frac{1}{8\pi i} \oint_C ds \frac{1}{\sqrt{s}} \ln \left( 1 - \frac{\omega_0 g}{N} \sum_{\mathbf{q}} \frac{\Omega_{\mathbf{q}}}{s - \Omega_{\mathbf{q}}^2} \right). \quad (42)$$

The summation over  $\mathbf{q}$  is performed within the first Brillouin zone over sites of the reciprocal lattice with the number of sites  $N = \frac{V}{a_0^3} = (2l)^3$  (with  $L \equiv 2la_0$ ). Thus the present treatment is in fact for the lattice polaron rather than for the continuum polaron in bulk. The subsequent numeric check shows that the relative difference between the energies for the continuum and lattice polarons becomes negligibly small already at relatively small  $l$ . For example, the relative difference of the ground state energies calculated with  $l = 10$  and  $l = 20$  is about  $2.4 \times 10^{-9}$ . Consequently, the lattice representation very well reproduces the properties of a polaron in bulk even at relatively small number of sites.

To obtain the particular case of the atomic limit (AL), the limiting transition  $t \rightarrow 0$  can be taken explicitly for the leading term of the ground state energy. For the ground state energy in this limit we can consider the Hamiltonian

$$\lim_{t \rightarrow 0} H_0 = \sum_{\mathbf{q}} \omega_0 \left( b_{\mathbf{q}}^\dagger b_{\mathbf{q}} + \frac{1}{2} \right) + \frac{\omega_0 g}{4N} \left( \sum_{\mathbf{q}} (b_{\mathbf{q}} + b_{\mathbf{q}}^\dagger) \right)^2. \quad (43)$$

For the numeric calculation, we apply the expression (42), which is simplified in the atomic limit to the analytic expression for the ground-state energy, which is exact for (43):

$$\begin{aligned} \Delta E_0^{(AL)} &= -\frac{\omega_0}{4\pi i} \oint_C dz \ln \left( 1 - \frac{g}{z^2 - 1} \right) \\ &= \frac{1}{2} \omega_0 \left( \sqrt{g+1} \Theta(g+1) - 1 \right), \end{aligned} \quad (44)$$

where  $\Theta(g+1)$  is the Heaviside step function. Equivalently, the Hamiltonian (43) can be exactly diagonalized by the Bogoliubov-Tyablikov canonical transformation similarly to (39). In the atomic limit, the value  $g = -1$  indicates the polaron instability as discussed above and in Ref. [15].

In Fig. 6 (a), we plot the ground state polaron energy of a polaron with a quadratic interaction as a function of the coupling constant  $g$  in the adiabatic regime, with  $\omega_0 = 0.25t$ . The obtained ground state energy is compared with the DiagMC data of Ref. [15] shown by full dots.

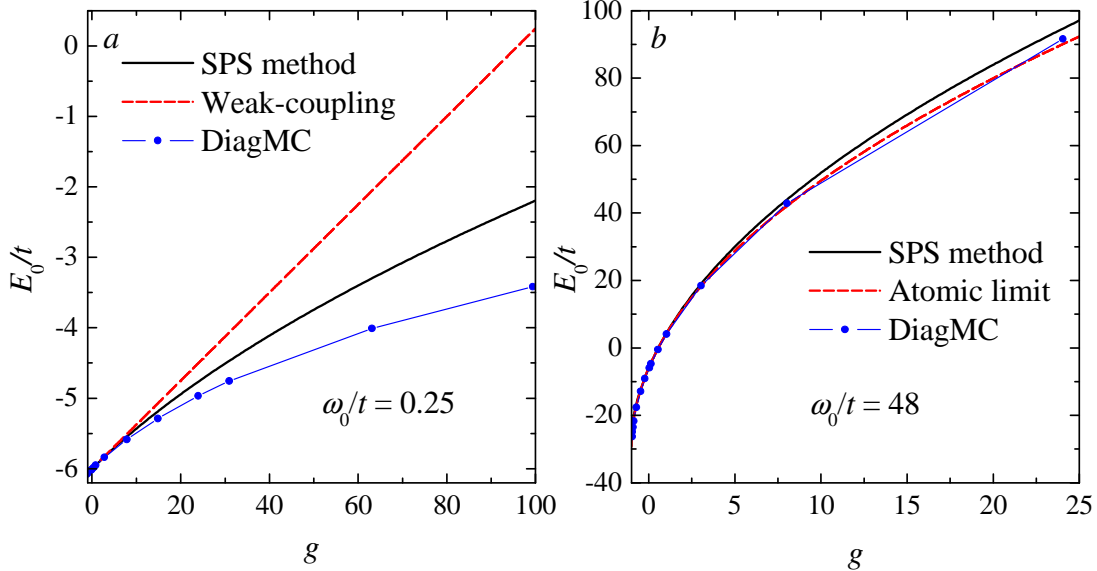


FIG. 6: Ground state energy of the quadratic polaron in the adiabatic regime with  $\omega_0 = 0.25t$  (a) and in the antiadiabatic regime with  $\omega_0 = 48t$  (b) as a function of the strength  $g$  of the quadratic electron-phonon coupling calculated within the present approach (solid curve) and by DiagMC (dots). The DiagMC data are from Ref. [15]. In the panel (a), the dashed line shows the weak-coupling limit for the ground state energy within the first-order perturbation theory. In the panel (b), the dashed curve shows the ground-state energy in the atomic limit  $t \rightarrow 0$  calculated using the expression (44).

As we can see from Fig. 6 (a), the qualitative behavior of the ground state energy within the extended squeezed phonon approach is similar to that obtained using DiagMC calculations. In the adiabatic regime the extension of the squeezed phonon method to the polaron in the tight-binding conduction band provides polaron ground state energy values in between the weak-coupling results and the DiagMC data, being closer to DiagMC rather than to the weak-coupling result. For a weak and intermediate coupling strength ( $g \lesssim 10$ ), the agreement between the squeezed phonon approximation and DiagMC results seems to be rather good.

In Fig. 6 (b), the ground state energy is calculated for  $\omega_0/t = 48$ , which corresponds to the antiadiabatic regime. In the antiadiabatic regime, when  $\omega_0 \gg t$ , the agreement between the current method with squeezed phonon states and DiagMC for the ground state energy appears to be better than in the adiabatic regime. This is explained by the fact that in the

limit  $t \rightarrow 0$ , the coordinate-free Hamiltonian (35) tends to a quadratic form which is *exactly* diagonalized by the Bogoliubov-Tyablikov transformation. For the comparison, the result of this limiting transition is shown by the red dashed curve in Fig. 6 (b). The ground state energy calculated using the approximation of squeezed phonon states consistently registers higher values compared to the results derived from the full DiagMC series, as distinct from the partial DiagMC summation in Sec. II. This trend is not observed in the atomic limit in comparison with DiagMC results due to the finite width of the conduction band. Under strong coupling conditions, the ground state energy within the atomic limit may fall below the DiagMC results for  $t \neq 0$ , as depicted in Fig. 6 (b).

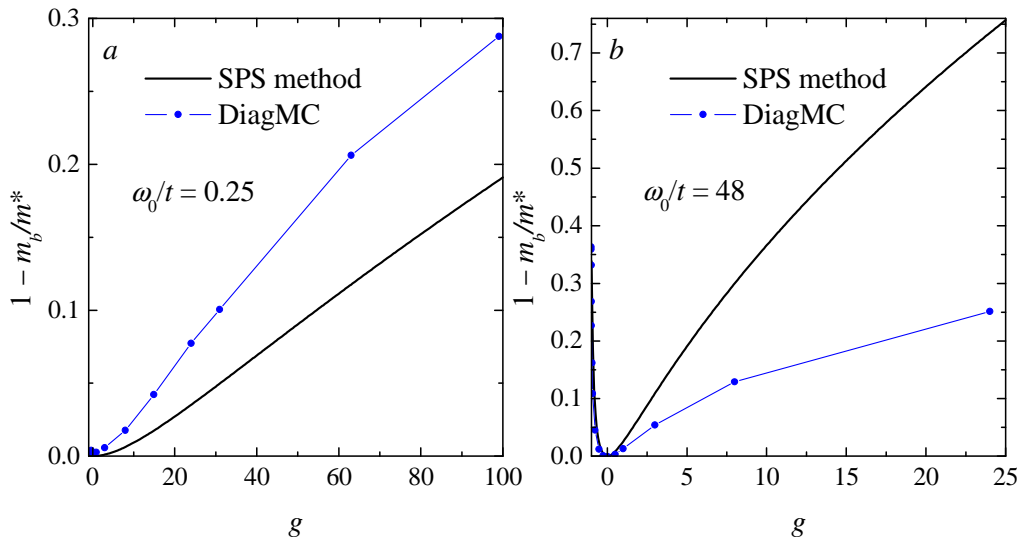


FIG. 7: Parameter  $\kappa = 1 - m_b/m^*$  of the quadratic polaron in the adiabatic regime with  $\omega_0 = 0.25t$  (a) and in the antiadiabatic regime with  $\omega_0 = 48t$  (b) as a function of the coupling strength  $g$  calculated using the SPS method (solid curves) and by DiagMC, Ref. [15] (dots).

In Fig. 7, we plot the parameter  $\kappa = 1 - m_b/m^*$  which determines the polaron effective mass  $m^*$ , in the adiabatic (a) and antiadiabatic (b) regimes. The parameter  $\kappa$  is the coefficient at  $k^2$  in the series expansion of the momentum-dependent polaron energy  $E_p(\mathbf{k})$  in powers of  $\mathbf{k}$ . For the simple cubic tight-binding band used in the present work and in Ref. [15], the electron and polaron effective masses are isotropic.

The dependence of  $\kappa$  as a function of the coupling constant  $g$  is qualitatively similar to that extracted from the DiagMC data. However, quantitatively there is a difference between our results and Ref. [15]. In the adiabatic regime, the present calculation underestimates

the polaron mass with respect to the DiagMC result. On the contrary, in the antiadiabatic regime we can see an overestimation of  $\kappa$  given by the present method with respect to DiagMC.

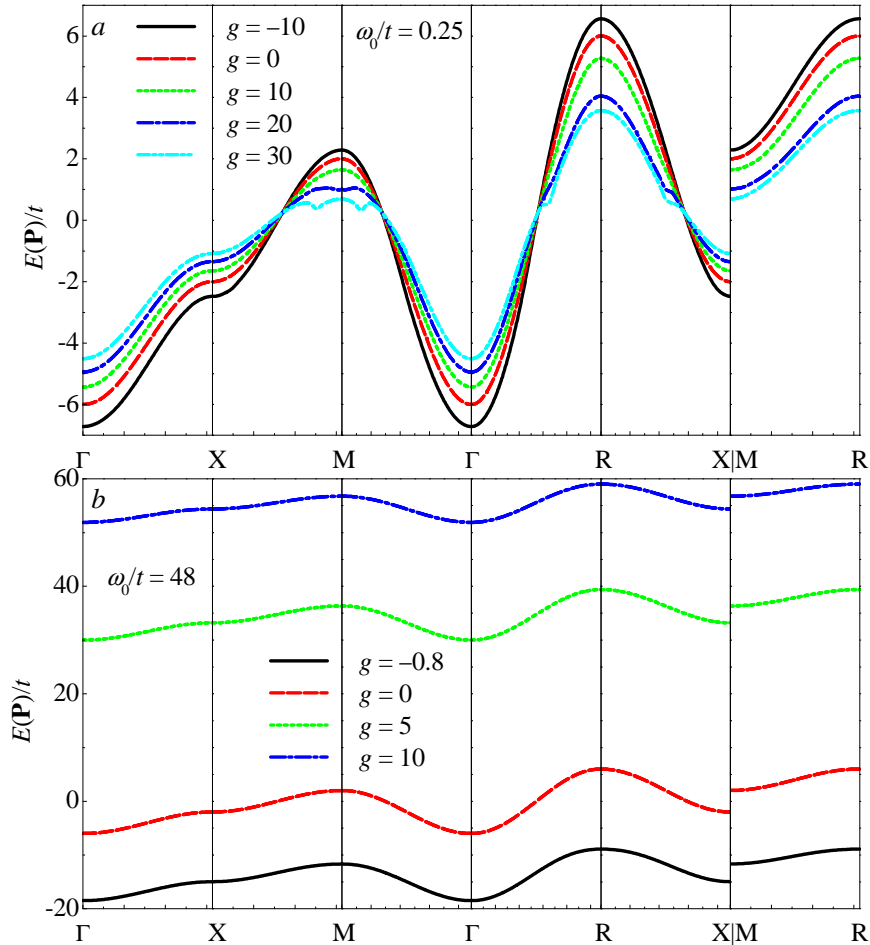


FIG. 8: Band dispersion of the polaron with a quadratic interaction in the adiabatic case with  $\omega_0/t = 0.25$  (a) and in the antiadiabatic case with  $\omega_0/t = 48$  (b) along the path for the cubic lattice  $\Gamma - X - M - \Gamma - R - X|M - R$  for different values of the coupling strength.

Because the approximated coordinate-free Hamiltonian keeps the translation symmetry of the initial electron-phonon Hamiltonian, it allows us to calculate the polaron energy  $E_p(\mathbf{k})$  in the whole Brillouin zone. In Fig. 8 (a), the band dispersion is shown for the polaron with a quadratic interaction for several values of the coupling constant  $g$  (including  $g = 0$  which corresponds to the bare band electron) along the standard path for the cubic lattice:  $\Gamma - X - M - \Gamma - R - X|M - R$  in the adiabatic regime with  $\omega_0/t = 0.25$ . As can be seen from the figure, the quadratic electron-phonon interaction leads to a narrowing of the conduction

band with respect to that of the bare electron. For sufficiently high coupling strengths, the polaron self-energy exhibits non-monotonic behavior at large momentum close to the point  $M$ , so that local minima appear along the chosen path. Consequently, the polaron band dispersion is more complicated than the electron band dispersion.

The polaron band dispersion in the antiadiabatic regime shown in Fig. 8 (*b*) looks differently from the momentum-dependent energy in the adiabatic regime. First, here the polaron shift of the energy is relatively large with respect to the electron bandwidth. As a result, the polaron effect on the energy in the antiadiabatic regime is expressed through the shift of the whole band rather than through a renormalization of the bandwidth. Thus in the antiadiabatic regime the top and the bottom of the conduction band shift in the same directions, while in the adiabatic case they shift in the opposite directions.

Looking back at Figs 6(*b*) and 7(*b*), we can note that the method of squeezed phonon states is highly effective at approximating the ground-state energy in the deep anti-adiabatic regime, but it performs rather poorly in quantitatively estimating the effective mass. Observing the polaron dispersion in Fig. 8, we can conclude that in the deep antiadiabatic regime the intraband dispersion of the polaron self-energy (as well the conduction band width) is small with respect to the shift of the whole band. The good agreement between the method of squeezed phonon states and DiagMC on the ground-state energy in the deep antiadiabatic regime is explained by the fact that the expression (43) represents the atomic limit not only for the truncated Hamiltonian (39) but also for the exact one (35). As the variation of the polaron self-energy within the conduction band in the deep antiadiabatic regime constitutes only a small part of the total self-energy, the relative error for the effective mass in this regime can be substantially larger than for the ground-state energy. Despite this quantitative deviation from the DiagMC results, the method of squeezed phonon states rather well captures the behavior of the effective mass at  $g < 0$  and the value of the critical negative coupling strength indicating the polaron instability.

#### IV. CONCLUSIONS

One of the primary outcomes of this treatment involves incorporating quadratic electron-phonon interaction into the squeezed phonon states scheme, which appears straightforward. The resulting dependence of the ground state energy and the effective mass of a polaron,

arising from the quadratic interaction between an electron and TO-phonons, exhibits notable differences for positive and negative coupling constants. In the regime of positive coupling strengths, we observe behavior typical of a repulsive polaron, without irregularities. However, for a negative coupling constant, the polaron's effective mass diverges at a critical value of the negative coupling strength. This divergence indicates a polaron instability, akin to what has been described in Ref. [15].

An advantageous feature of the current modification to the squeezed phonon states method lies in its ability to calculate the polaron band dispersion across the entire Brillouin zone, extending beyond the assumption of small polaron momentum and the quadratic expansion in powers of polaron momentum, and keeping the periodic boundary conditions exactly. This represents the second key result of our present work.

Even for a parabolic band, achieving a comprehensive variational treatment is inherently complex [6]. The feasibility of obtaining a tractable form for the complete correlated Gaussian wavefunction remains uncertain in the context of a nonparabolic conduction band. This unresolved question serves as the focus of subsequent studies.

The analytic method employed in this work enables the investigation of various polaron characteristics across a broad range of parameters, including coupling strength. Notably, it complements the numeric DiagMC treatment. Our method's predictions align qualitatively with DiagMC results, highlighting features such as the instability of the polaron with quadratic interaction at specific negative coupling strengths.

## **Acknowledgments**

This work is supported financially by the Research Foundation - Flanders, projects GOH1122N, G061820N, G060820N, and by the University Research Fund (BOF) of the University of Antwerp. MH acknowledges funding by Research Foundation - Flanders via a postdoc fellowship (grant 1224724N). Financial support from the Austrian Science Fund (FWF) Project No. I 4506 (FWO- FWF joint project) is gratefully acknowledged. ASM acknowledges the support of the FrustKor project financed by the European Union through the National Recovery and Resilience Plan 2021-2026 (NRPP) and JSPS KAKENHI Grant Kiban A:24H00197.

## Appendix A: Derivation of the polaron self-energy

The off-diagonal component of the quadratic Hamiltonian (11) and (39) remains irrelevant to the energy within the Lee-Low-Pines approximation. The Bogoliubov-Tyablikov canonical transformation, as described in [24, 28, 29], is the third transformation,

$$\begin{aligned} b_{\mathbf{q}}^{(a)} &= \frac{1}{\sqrt{V}} \sum_{\mathbf{q}', a'} \left( u_{\mathbf{q}\mathbf{q}'}^{(aa')} \beta_{\mathbf{q}'}^{(a')} + v_{\mathbf{q}\mathbf{q}'}^{(aa')*} \beta_{\mathbf{q}'}^{(a')\dagger} \right), \\ b_{\mathbf{q}}^{(a)\dagger} &= \frac{1}{\sqrt{V}} \sum_{\mathbf{q}', a'} \left( u_{\mathbf{q}\mathbf{q}'}^{(aa')*} \beta_{\mathbf{q}'}^{(a')\dagger} + v_{\mathbf{q}\mathbf{q}'}^{(aa')} \beta_{\mathbf{q}'}^{(a')} \right). \end{aligned} \quad (\text{A1})$$

This mixes the creation and annihilation phonon operators, and corresponds to a transformation from the original phonon states to squeezed phonon states. This is why we refer to this approach as the “squeezed phonon state” approach. When the Bogoliubov-Tyablikov transformation is used in conjunction with the displacement operator  $S_2$ , this leads to displaced squeezed phonon states, which are useful when both a linear-harmonic interaction and a quadratic interaction are present. The matrix elements of the Bogoliubov-Tyablikov unitary transformation are chosen in order to diagonalize the Hamiltonian  $H_0$ . After applying (A1) to (39), the resulting Hamiltonian can be written as:

$$H_0 = E_0 + \sum_{a, \mathbf{q}} \hbar \nu_{\mathbf{q}}^{(a)} \beta_{\mathbf{q}}^{(a)\dagger} \beta_{\mathbf{q}}^{(a)} + \Delta E, \quad (\text{A2})$$

where  $\nu_{\mathbf{q}}^{(a)}$  are eigenfrequencies, and  $\Delta E$  is the polaron energy shift,

$$\Delta E = \frac{1}{2} \sum_{a, \mathbf{q}} \hbar (\nu_{\mathbf{q}}^{(a)} - \Omega_{\mathbf{q}}^{(a)}). \quad (\text{A3})$$

In order to obtain the polaron self-energy within the squeezed phonon states method for  $H_0$ , we do not need an explicit form of eigenfrequencies and matrix elements. The self-energy can be derived using a scheme described by Wentzel [31]. First, the Hamiltonian  $H_0$  is rewritten in terms of phonon coordinates and momenta,

$$\begin{aligned} Q_{\mathbf{q}}^{(a)} &= \sqrt{\frac{\hbar}{2m\Omega_{\mathbf{q}}^{(a)}}} (b_{\mathbf{q}}^{(a)\dagger} + b_{\mathbf{q}}^{(a)}) \\ P_{\mathbf{q}}^{(a)} &= -i\sqrt{\frac{\hbar m\Omega_{\mathbf{q}}^{(a)}}{2}} (b_{\mathbf{q}}^{(a)} - b_{\mathbf{q}}^{(a)\dagger}) \end{aligned} \quad (\text{A4})$$



leading to

$$H_0 = E_0 + \sum_{a,\mathbf{q}} \left( \frac{(P_{\mathbf{q}}^{(a)})^2}{2m} + \frac{m(\Omega_{\mathbf{q}}^{(a)})^2}{2} (Q_{\mathbf{q}}^{(a)})^2 \right) + \hbar \mathbf{W}_1^2 + \frac{g_2 m}{\hbar} \mathbf{W}_2^2 - \frac{1}{2} \sum_{a,\mathbf{q}} \hbar \Omega_{\mathbf{q}}^{(a)}, \quad (\text{A5})$$

with the collective coordinates

$$\mathbf{W}_1 = \sum_{a,\mathbf{q}} \mathbf{q} \sqrt{\Omega_{\mathbf{q}}^{(a)}} f_{\mathbf{q}}^{(a)} Q_{\mathbf{q}}^{(a)}, \quad \mathbf{W}_2 = \sum_{\mathbf{q},a=1,2} \frac{\mathbf{e}_{\mathbf{q}}^{(a)} \varkappa_{\mathbf{q}} \sqrt{\Omega_{\mathbf{q}}^{(a)}}}{\sqrt{V}} Q_{\mathbf{q}}^{(a)}. \quad (\text{A6})$$

The equation for eigenfrequencies and eigenvectors of the quadratic form (A5) is determined in the standard way:

$$\sum_{a',\mathbf{q}'} M_{\mathbf{q}',\mathbf{q}}^{(a,a')}(\omega) Q_{\mathbf{q}'}^{(a')}(\omega) = 0, \quad (\text{A7})$$

where the elements of the matrix  $\mathbb{M}(\omega) = \left\| M_{\mathbf{q}',\mathbf{q}}^{(a,a')}(\omega) \right\|$  are

$$M_{\mathbf{q}',\mathbf{q}}^{(a,a')}(\omega) = \delta_{a',a} \delta_{\mathbf{q}',\mathbf{q}} \left[ \omega^2 - (\Omega_{\mathbf{q}}^{(a)})^2 \right] - 2\hbar (\mathbf{q} \otimes \mathbf{q}') \sqrt{\Omega_{\mathbf{q}}^{(a)} \Omega_{\mathbf{q}'}^{(a')}} f_{\mathbf{q}}^{(a)} f_{\mathbf{q}'}^{(a')} - (1 - \delta_{a,3}) (1 - \delta_{a',3}) \frac{2g_2}{\hbar V} \left( \mathbf{e}_{\mathbf{q}}^{(a)} \otimes \mathbf{e}_{\mathbf{q}'}^{(a')} \right) \varkappa_{\mathbf{q}} \varkappa_{\mathbf{q}'} \sqrt{\Omega_{\mathbf{q}}^{(a)} \Omega_{\mathbf{q}'}^{(a')}}. \quad (\text{A8})$$

The eigenfrequencies are the roots of the equation

$$\det \mathbb{M}(\omega) = 0. \quad (\text{A9})$$

A reduced set of equations for collective coordinates (A6) can be extracted from the full set of equations (A7) when we divide the equation by  $\left[ \omega^2 - (\Omega_{\mathbf{q}}^{(a)})^2 \right]$  and perform summations over  $\mathbf{q}$  with different weight coefficients. It results in the matrix equation

$$\mathbb{A}(\omega) \mathbf{W}(\omega) = 0, \quad (\text{A10})$$

where  $\mathbf{W}(\omega)$  is a 6-dimensional vector, which is given in a block form by:

$$\mathbf{W}(\omega) = \begin{pmatrix} \mathbf{W}_1(\omega) \\ \mathbf{W}_2(\omega) \end{pmatrix}.$$

The matrix  $\mathbb{A}(\omega)$  can be written as the block matrix

$$\mathbb{A}(\omega) = \begin{pmatrix} \mathbb{A}^{(\text{LO})}(\omega) & \mathbb{A}^{(\text{mix})}(\omega) \\ [\mathbb{A}^{(\text{mix})}(\omega)]^T & \mathbb{A}^{(\text{2TO})}(\omega) \end{pmatrix}, \quad (\text{A11})$$

with the matrices

$$\mathbb{A}^{(\text{LO})}(\omega) = \mathbb{I} - 2\hbar \sum_{\mathbf{q}, a=1,2,3} \alpha_{\mathbf{q}}^{(a)}(\mathbf{q} \otimes \mathbf{q}), \quad (\text{A12})$$

$$\mathbb{A}^{(2\text{TO})}(\omega) = \mathbb{I} - \frac{2g_2}{\hbar V} \sum_{\mathbf{q}, a=1,2} \lambda_{\mathbf{q}}^{(a)}(\mathbf{e}_{\mathbf{q}}^{(a)} \otimes \mathbf{e}_{\mathbf{q}}^{(a)}), \quad (\text{A13})$$

$$\mathbb{A}^{(\text{mix})}(\omega) = -\frac{2g_2}{\hbar\sqrt{V}} \sum_{\mathbf{q}, a=1,2} \gamma_{\mathbf{q}}^{(a)}(\mathbf{q} \otimes \mathbf{e}_{\mathbf{q}}^{(a)}), \quad (\text{A14})$$

and weight functions

$$\alpha_{\mathbf{q}}^{(a)}(\omega) = \frac{\Omega_{\mathbf{q}}^{(a)} \left(f_{\mathbf{q}}^{(a)}\right)^2}{\omega^2 - \left(\Omega_{\mathbf{q}}^{(a)}\right)^2}, \lambda_{\mathbf{q}}^{(a)}(\omega) = \frac{\varkappa_{\mathbf{q}}^2 \Omega_{\mathbf{q}}^{(a)}}{\omega^2 - \left(\Omega_{\mathbf{q}}^{(a)}\right)^2}, \gamma_{\mathbf{q}}^{(a)}(\omega) = \frac{\varkappa_{\mathbf{q}} \Omega_{\mathbf{q}}^{(a)} f_{\mathbf{q}}^{(a)}}{\omega^2 - \left(\Omega_{\mathbf{q}}^{(a)}\right)^2}. \quad (\text{A15})$$

The eigenvalues of the phonon energy are determined by the equation

$$\det \mathbb{A}(\omega) = 0. \quad (\text{A16})$$

A mixing of the Fröhlich and 2TO interactions is provided by non-diagonal blocks of the matrix (A11). For  $P = 0$ , they are exactly equal to zero due to symmetry. Therefore, for the ground-state energy the Fröhlich and 2TO contributions are completely decoupled within the approach of squeezed phonon states. For a nonzero momentum, this mixing is not equal to zero. However, it can be significant only when the LO and TO phonon frequencies are in resonance. For soft TO phonon modes in strongly polar crystals like SrTiO<sub>3</sub>, this is not the case, and hence the aforesaid LO-TO phonon mixing is expected to be of a relatively small importance. When the non-diagonal blocks of  $\mathbb{A}(\omega)$  are neglected, it is reduced to a quasi-diagonal form of two blocks describing, respectively, Fröhlich and 2TO contributions. Without loss of generality, we can choose axes in coordinate and momentum spaces such that  $\mathbf{P} \parallel Oz$ , so that  $P_z = P, P_x = P_y = 0$ . In this basis, the first block is:

$$\mathbb{A}^{(\text{LO})}(\omega) = \begin{pmatrix} A_{xx} & 0 & 0 \\ 0 & A_{yy} & 0 \\ 0 & 0 & A_{zz} \end{pmatrix}$$

with the matrix elements

$$A_{jj} = 1 - 2\hbar \sum_{\mathbf{q}, a=1,2,3} \alpha_{\mathbf{q}}^{(a)} k_j^2. \quad (\text{A17})$$

Also the second block results in the diagonal matrix:

$$\mathbb{A}^{(2\text{TO})}(\omega) = \begin{pmatrix} B_{xx} & 0 & 0 \\ 0 & B_{yy} & 0 \\ 0 & 0 & B_{zz} \end{pmatrix} \quad (\text{A18})$$

with the matrix elements:

$$B_{jj} = 1 - \frac{g_2}{\hbar V} \sum_{\mathbf{q}, a=1,2} \lambda_{\mathbf{q}}^{(a)} \left( 1 - \frac{k_j^2}{k^2} \right). \quad (\text{A19})$$

As the Fröhlich polaron self-energy within the approach of squeezed phonon states is already thoroughly studied in the literature [6, 25, 28–30], we focus on the contribution for the polaron self-energy for a 2TO interaction. The determinant of the matrix  $\mathbb{A}^{(2\text{TO})}(\omega)$  is

$$\det \mathbb{A}^{(2\text{TO})}(\omega) = \prod_{j=x,y,z} \left( 1 - \frac{g_2}{\hbar V} \sum_{\mathbf{q}, a=1,2} \lambda_{\mathbf{q}}^{(a)} \left( 1 - \frac{k_j^2}{k^2} \right) \right). \quad (\text{A20})$$

The change in the self-energy resulting from the Bogoliubov-Tyablikov diagonalization is established in the following manner, following the logical framework outlined in Ref. [31]. The eigenfrequencies are solutions to the equation

$$\det \mathbb{M}(\omega) = 0. \quad (\text{A21})$$

The matrix  $\mathbb{M}(\omega)$  is diagonalized using the Bogoliubov-Tyablikov transformation described above. The transformation (A1) is unitary and can be written as  $\mathbb{U}_{\text{BT}} F(b^\dagger, b) \mathbb{U}_{\text{BT}}^{-1}$  for any function of phonon operators  $F(b^\dagger, b)$ . Hence, the diagonalized matrix is

$$\tilde{\mathbb{M}}(\omega) = \mathbb{U}_{\text{BT}} \mathbb{M}(\omega) \mathbb{U}_{\text{BT}}^{-1} = \left\| \delta_{a',a} \delta_{\mathbf{q}',\mathbf{q}} \left[ \omega^2 - (\nu_{\mathbf{q}}^{(a)})^2 \right] \right\| \quad (\text{A22})$$

where  $\nu_{\mathbf{q}}^{(a)}$  are eigenfrequencies. The determinant of the matrix  $\mathbb{M}(\omega)$  is an invariant of unitary transformations:  $\det \tilde{\mathbb{M}}(\omega) = \det \mathbb{M}(\omega)$ . Hence

$$\det \mathbb{M}(\omega) = \prod_{a,\mathbf{q}} \left[ \omega^2 - (\nu_{\mathbf{q}}^{(a)})^2 \right]. \quad (\text{A23})$$

If the interaction terms in (A8) tend to zero, this determinant turns to its limiting value

$$\det \mathbb{M}_0(\omega) = \prod_{a,\mathbf{q}} \left[ \omega^2 - (\Omega_{\mathbf{q}}^{(a)})^2 \right]. \quad (\text{A24})$$

Let us introduce the ratio function of  $s \equiv \omega^2$ :

$$\Delta(s) \equiv \prod_{a,\mathbf{q}} \frac{s - \left(\nu_{\mathbf{q}}^{(a)}\right)^2}{s - \left(\Omega_{\mathbf{q}}^{(a)}\right)^2} = \frac{\det \mathbb{M}(\omega)}{\det \mathbb{M}_0(\omega)}. \quad (\text{A25})$$

Eigenfrequencies  $\nu_{\mathbf{q}}^{(a)}$  are the solutions of Eq. (A9) and also satisfy the equation (A20):

$$\det \mathbb{A}(\omega) = 0. \quad (\text{A26})$$

Consequently,  $\det \mathbb{M}(\omega) \propto \det \mathbb{A}(\omega)$ . Using (A24) and the fact that  $\det \mathbb{A}(\omega)|_{\{f_k\}=0, g_2=0} = 1$ , we find that

$$\det \mathbb{M}(\omega) = \det \mathbb{M}_0(\omega) \det \mathbb{A}(\omega). \quad (\text{A27})$$

Consequently, we reproduced here the Wentzel result:

$$\Delta(\omega^2) = \det \mathbb{A}(\omega). \quad (\text{A28})$$

The polaron self-energy  $\Delta E$  is expressed through the function  $\Delta(s)$  using the identity [31]:

$$\frac{\partial}{\partial s} \ln \Delta(s) = \sum_{a,\mathbf{q}} \left( \frac{1}{s - \nu_{\mathbf{q}}^{(a)2}} - \frac{1}{s - \Omega_{\mathbf{q}}^{(a)2}} \right). \quad (\text{A29})$$

For any analytic function  $F(s)$  this can be expressed via the Cauchy integral formula as

$$\sum_{a,\mathbf{q}} (F(\nu_{\mathbf{q}}^{(a)2}) - F(\Omega_{\mathbf{q}}^{(a)2})) = -\frac{1}{2\pi i} \oint_C ds \frac{\partial F(s)}{\partial s} \ln \Delta(s), \quad (\text{A30})$$

where the contour  $C$  embraces all points  $s = \nu_{\mathbf{q}}^{(a)2}$  and  $s = \Omega_{\mathbf{q}}^{(a)2}$  as shown in Fig. 1, and the path direction along the contour is counterclockwise.

For the self-energy,  $F(s) = \sqrt{s}$ . Because the contour  $C$  lies in the area where  $\text{Re } s > 0$ ,  $\sqrt{s}$  is an analytic single-valued function in that region. Hence

$$\Delta E = -\frac{\hbar}{8\pi i} \oint_C ds \frac{1}{\sqrt{s}} \ln \Delta(s) \quad (\text{A31})$$

where the factor  $\Delta(s)$  is related to the matrix  $\mathbb{A}$  as

$$\Delta(\omega^2) = \det \mathbb{A}(\omega). \quad (\text{A32})$$

The particular 2TO contribution to the polaron energy is then

$$\Delta E^{(2\text{TO})} = -\frac{\hbar}{8\pi i} \oint_C ds \frac{1}{\sqrt{s}} \ln \Delta^{(2\text{TO})}(s), \quad (\text{A33})$$

$$\Delta^{(2\text{TO})}(s) = \prod_{j=x,y,z} \left( 1 - \frac{g_2}{\hbar V} \sum_{\mathbf{q}, a=1,2} \frac{\varkappa_{\mathbf{q}}^2 \Omega_{\mathbf{q}}^{(a)}}{s - \left(\Omega_{\mathbf{q}}^{(a)}\right)^2} \left( 1 - \frac{k_j^2}{k^2} \right) \right). \quad (\text{A34})$$

This is equation (18) from the main text.

## Appendix B: Diagrammatic Monte Carlo for the 2TO interaction

The DiagMC method employed to obtain the polaron energies for the 2TO interaction in Fig. 3 (b) is largely based on the section *Momentum space representation* in Ref. [15] and further described in its Supplemental Material.

Consider the Hamiltonian in Eq. 1. Assuming a symmetric choice for the polarization vectors such that  $\mathbf{e}_{\mathbf{q}}^{(1)} = \mathbf{e}_{-\mathbf{q}}^{(1)}$  and  $\mathbf{e}_{\mathbf{q}}^{(2)} = \mathbf{e}_{-\mathbf{q}}^{(2)}$ ,  $H_{2\text{TO}}$  can be expressed in the form

$$H_{2\text{TO}} = \sum_{\mathbf{k}, \mathbf{q}, \mathbf{q}', a, a'} V_{\mathbf{q}, \mathbf{q}'}^{(a, a')} a_{\mathbf{k}+\mathbf{q}+\mathbf{q}'}^\dagger a_{\mathbf{k}} (b_{-\mathbf{q}}^{(a)\dagger} + b_{\mathbf{q}}^{(a)}) (b_{-\mathbf{q}'}^{(a')\dagger} + b_{\mathbf{q}'}^{(a')}) \quad (\text{B1})$$

which is the same as in Ref. [15, Suppl. material, Eq. 17]. The constant vertex  $(g_2\Omega/4)/(2\pi)^3$  is replaced by

$$V_{\mathbf{q}, \mathbf{q}'}^{(a, a')} = \frac{1}{(2\pi)^3} \frac{3\pi^2 \alpha_T}{4} \frac{\mathbf{e}_{\mathbf{q}}^{(a)} \cdot \mathbf{e}_{\mathbf{q}'}^{(a')}}{\sqrt{\omega_{\text{TO}}^{(a)}(\mathbf{q}) \omega_{\text{TO}}^{(a')}(\mathbf{q}')}}, \quad (\text{B2})$$

with the following choice of polarization vectors

$$\mathbf{e}_{\mathbf{q}}^{(1)} = \mathbf{e}_{\mathbf{q}}^\theta = \left( \cos(\theta) \cos(\phi), \cos(\theta) \sin(\phi), -\sin(\theta) \right) \quad (\text{B3})$$

$$\mathbf{e}_{\mathbf{q}}^{(2)} = \mathbf{e}_{\mathbf{q}}^\phi = \left( -\sin(\phi), \cos(\phi), 0 \right) \cdot \text{sgn}(\cos(\theta)) \quad (\text{B4})$$

where

$$\theta = \arccos(q_z/q) \quad (\text{B5})$$

$$\phi = \arctan(q_y/q_x). \quad (\text{B6})$$

In order to impose a momentum cutoff, every time a phonon momentum is to be extracted in the MC updates, it is chosen uniformly inside a sphere in momentum space with radius  $k_0$ . Consequently, the acceptance ratio of the *Add/remove 2-loop* and *Add/remove 3-loop* updates must be modified to contain, respectively,  $U(\mathbf{q}_1, \mathbf{q}_2) = (4/3\pi k_0^3)^{-2}$  and  $U(\mathbf{q}_1, \mathbf{q}_2, \mathbf{q}_3) = (4/3\pi k_0^3)^{-3}$ . The uniform choice of a particular polarization for the inserted phonon yields a further probability factor of 1/4 (2-loop) or 1/8 (3-loop) that must be taken into account in the acceptance ratio.

The summation of the complete series of 1-loop diagrams can be analytically calculated and corresponds precisely to the first order energy correction (21). As in Ref. [15], to

alleviate the sign problem in the positive coupling regime, these diagrams can be included into a renormalized electron propagator with a dispersion shifted by (21).

- 
- [1] R. P. Feynman, *Statistical Mechanics: A Set Of Lectures*, Westview Press (1998).
  - [2] A. S. Alexandrov and J. T. Devreese, *Advances in Polaron Physics*, (Springer Series in Solid State Science vol. 159, Springer Berlin, Heidelberg, 2009); see also J. T. Devreese, *Fröhlich Polarons. Lecture course including detailed theoretical derivations*, <https://arxiv.org/abs/1611.06122> for an detailed review on polaron physics.
  - [3] C. Franchini, M. Reticcioli, M. Setvin, U. Diebold, “Polarons in Materials ”, *Nat. Rev. Mater.* **6**, 560-586 (2021).
  - [4] A. Schirotzek, C.-H. Wu, A. Sommer, and M. W. Zwierlein, “Observation of Fermi Polarons in a Tunable Fermi Liquid of Ultracold Atoms”, *Phys. Rev. Lett.* **102**, 230402 (2009).
  - [5] C. Kohstall, M. Zaccanti, M. Jag, A. Trenkwalder, P. Massignan, G. M. Bruun, F. Schreck, and R. Grimm, “Metastability and coherence of repulsive polarons in a strongly interacting Fermi mixture”, *Nature* **485**, 615 (2012).
  - [6] Yu. E. Shchadilova, F. Grusdt, A. N. Rubtsov, and E. Demler, “Polaronic mass renormalization of impurities in BEC: correlated Gaussian wavefunction approach”, *Phys. Rev. A* **93**, 043606 (2016).
  - [7] M. Kutschera and W. Wójcik, “Proton impurity in the neutron matter: A nuclear polaron problem”, *Phys. Rev. C* **47**, 1077 (1993).
  - [8] S. Nascimbène, N. Navon, K. J. Jiang, F. Chevy, and C. Salomon, “Exploring the thermodynamics of a universal Fermi gas”, *Nature* **463**, 1057 (2010).
  - [9] J. Tempere, W. Casteels, M.K. Oberthaler, E. Timmermans, J.T. Devreese “Feynman path-integral treatment of the BEC-impurity polaron ”*Phys. Rev. B* **80**, 184504 (2009).
  - [10] Y. N. Epifanov, A. P. Levanyuk, and G. M. Levanyuk, “Interaction of carriers with TO-phonons and electrical conductivity of ferroelectrics”, *Ferroelectrics* **35**, 199 (1981).
  - [11] L. Ranalli, C. Verdi, L. Monacelli, G. Kresse, M. Calandra, C. Franchini, “Temperature-Dependent Anharmonic Phonons in Quantum Paraelectric  $\text{KTaO}_3$  by First Principles and Machine-Learned Force Fields ”, *Adv. Quantum Technol.* 2200131 (2023).
  - [12] I. Errea, M. Calandra, C. J. Pickard, J. Nelson, R. J. Needs, Y. Li, H. Liu, Y. Zhang, Y. Ma,

- and F. Mauri, “High-pressure hydrogen sulfide from first principles: a strongly anharmonic phonon-mediated superconductor”, *Phys. Rev. Lett.* **114**, 157004 (2015).
- [13] A. Kumar , V. I. Yudson, and D. L. Maslov, “Quasiparticle and Nonquasiparticle Transport in Doped Quantum Paraelectrics”, *Phys. Rev. Lett.* **126**, 076601 (2021).
- [14] M. Houtput and J. Tempere, “Beyond the Frohlich Hamiltonian : path-integral treatment of large polarons in anharmonic solids ”, *Phys. Rev. B* **103**, 184306 (2021).
- [15] S. Ragni, T. Hahn, Z. Zhang, N. Prokof’ev, A. Kuklov, S. Klimin, M. Houtput, B. Svistunov, J. Tempere, N. Nagaosa, C. Franchini, and A. S. Mishchenko, “Polaron with quadratic electron-phonon interaction”, *Phys. Rev. B* **107**, L121109 (2023).
- [16] C. P. J. Adolphs and M. Berciu, “Single-polaron properties for double-well electron-phonon coupling”, *Phys. Rev. B* **89**, 035122 (2014).
- [17] Carla Verdi, Luigi Ranalli, Cesare Franchini, and Georg Kresse “Quantum paraelectricity and structural phase transitions in strontium titanate beyond density functional theory ”, *Phys. Rev. Materials* **7**, L030801 (2023).
- [18] A.-G. Kussow, “Large polaron in an anharmonic crystal lattice”, *Int. J. Mod. Phys B* **23**, 19–38 (2009).
- [19] D. van der Marel, F. Barantani, and C. W. Rischau, “Possible mechanism for superconductivity in doped SrTiO<sub>3</sub>”, *Phys. Rev. Research* **1**, 013003 (2019).
- [20] M. N. Gastiasoro, J. Ruhman, and R. M. Fernandes, “Superconductivity in dilute SrTiO<sub>3</sub>: A review”, *Ann. Phys.* **417**, 168107 (2020).
- [21] M. J. Schilcher, P. J. Robinson, D. J. Abramovitch, L. Z. Tan, A. M. Rappe, D. R. Reichman, and D. A. Egger, “The Significance of Polarons and Dynamic Disorder in Halide Perovskites”, *ACS Energy Letters* **6**, 2162-2173 (2021).
- [22] A. S. Mishchenko, N. V. Prokof’ev, A. Sakamoto, and B. V. Svistunov, “Diagrammatic quantum Monte Carlo study of the Fröhlich polaron”, *Phys. Rev. B* **62**, 6317 (2000).
- [23] T. Hahn, S. Klimin, J. Tempere, J. T. Devreese, and C. Franchini, “Diagrammatic Monte Carlo study of Fröhlich polaron dispersion in two and three dimensions ”, *Phys. Rev. B* **97**, 134305 (2018).
- [24] E. P. Gross, *Phys. Rev.* **100**, 1571 (1955).
- [25] B. S. Kandemir and T. Altanhan, *J. Phys. Condens. Matter* **6**, 4505 (1994).
- [26] T. D. Lee, F. E. Low, and D. Pines, “The Motion of Slow Electrons in a Polar Crystal ”*Phys.*

- Rev. **90**, 297 (1953).
- [27] S. V. Tyablikov, *Methods in the Quantum Theory of Magnetism*, Plenum Press, 1967.
- [28] A. V. Tulub, “Slow electrons in polar crystals”, Sov Phys. JETP **14**, 1301-1307 (1962). [Russian original: J. Exptl. Theoret. Phys. (U.S.S.R.) **41**, 1828-1838 (1961).]
- [29] A. V. Tulub, “Comments on polaron-phonon scattering theory”, Theoretical and Mathematical Physics **185**, 1533-1546 (2015). [Russian original: Teoreticheskaya i Matematicheskaya Fizika **185**, 199-212 (2015).]
- [30] M. Porsch and J. Röseler, “Recoil effects in the polaron problem”, Phys. Stat. Sol. **23**, 365 (1967).
- [31] G. Wentzel, “Zur Paartheorie der Kernkräfte”, Helv. Phys. Acta, **15**, 111 (1942).
- [32] Zhaoyu Han, Steven A. Kivelson, and Pavel A. Volkov, “Quantum Bipolaron Superconductivity from Quadratic Electron-Phonon Coupling”, Phys. Rev. Lett. **132**, 226001 (2024).
- [33] B. Gerlach and H. Löwen, “Analytical properties of polaron systems or: Do polaronic phase transitions exist or not?”, Rev. Mod. Phys. **63**, 63 (1991).
- [34] Chao Zhang, Nikolay V. Prokof’ev, and Boris V. Svistunov, “Peierls/Su-Schrieffer-Heeger polarons in two dimensions”, Phys. Rev. B **104**, 035143 (2021).
- [35] J. T. Devreese, S. N. Klimin, J. L. M. van Mechelen, and D. van der Marel, “Many-body large polaron optical conductivity in  $\text{SrTi}_{1-x}\text{Nb}_x\text{O}_3$ ”, Phys. Rev. B **81**, 125119 (2010).